

1 Response to Reviews for “The pH dependency of the boron isotopic composition of diatom opal
2 (Thalassiosira weissflogii) by Donald et al.

3 **Reviewer RC1 – Jan Fietzke**

4 We thank the reviewer for his comments and in particular his recognition that, while this manuscript
5 is a start of the exploitation of boron isotopes in diatoms, it is not the final word on the matter. We
6 respond to each of his comments in turn below.

7 RC1: “I had the opportunity to analyze cultured T. weissflogii samples for their boron isotopic
8 composition using LA-MC-ICPMS about 7 years ago. On average those analyses resulted in d11B of
9 14.0 +- 1.1 (1sd). Unfortunately, the results appeared too imprecise to be useful and never got
10 published... Nevertheless, the significant difference of both, own data and those reported in this
11 manuscript, is quite striking to me.”

12 This is indeed quite a difference, but without more detail it is hard for us to critically evaluate this
13 observation. However, we would like to point out that: (i) we carried out an extensive cleaning
14 protocol to remove residual organic material; (ii) we carried out an extensive investigation of our
15 protocol including ensuring little to no boron was lost during the purification process; and (iii) our
16 standard addition tests support the conclusion that our $\delta^{11}\text{B}$ analytical method is accurate. It is also
17 perhaps worth noting that all published $\delta^{11}\text{B}$ measurements to date are also isotopically light, like
18 our results – though we acknowledge that this is a rather limited dataset to make such comparisons.
19 In the future we would welcome engaging with the community to further explore the analytical
20 accuracy of $\delta^{11}\text{B}$ in opal-matrices by various analytical techniques.

21 RC1: “I would like to see in an additional figure a direct comparison of the [B] vs. pH systematic
22 reported by Meija et al. (2013) and this study.”

23 This was included in the original manuscript as a supplementary figure. Given this comment (and a
24 similar one by reviewer RC2) we have now brought this data into Figure 5 (grey circles).

25 RC1: “The authors suggest the differences may be due to the use of LA and conventional ICPMS. I do
26 not think, the LA results published by Meija et al. (2013) are inaccurate.”

27 This is not actually what we say in the manuscript, we were careful not to apportion cause and
28 instead we said the following: “In detail, however, our concentrations are around 2-3 times lower
29 than Meija et al. (2013), perhaps due to the different analytical methods used (laser ablation ICP-MS
30 vs. solution here...”.

31 RC1: “So, this would indicate three possibilities: a) samples for the older LA study had not been
32 cleaned sufficiently (which I doubt strongly) b) the sample preparation used in this study resulted in
33 a loss of boron or c) some details in the culturing setups resulted in this observable differences.”

34 Since we have not done a direct comparison of methods for determining B/Si it is hard to determine
35 the specific cause. However, given this comment, we now briefly discuss these possibilities in the
36 manuscript, expanding on the observed discrepancy (in absolute B/Si but not in the relationship
37 between B/Si and pH) in lines 289-292.

38 RC1: “I would also be interested to see a figure displaying d11B vs. [B]. From figure 5 it appears there
39 may be a stronger correlation of those two parameters than the ones of each of both vs. pH.”

40 There is in fact a weaker relationship between these two variables than between each and pH. We
41 therefore decided not to include this figure as it distracted from the good relationships with pH.

42 RC1: "The model proposed to explain the data (including the -10permil offset during incorporation
43 into opal) is not really satisfying... This would need a better, more detailed description, maybe
44 including a schematic figure for a better conceptual understanding."

45 We have now included a schematic (Figure 8) and have modified the relevant section to improve
46 clarity (also in accordance with the comments of RC2 below).

47

48 **Reviewer RC2 – Joji Uchikawa**

49 We thank this reviewer for his comments and we are pleased that he favours publication and
50 recognises the importance of this contribution. In order to harvest sufficient biomass from our
51 dilute batch cultures we had to let them continue longer than we would have if we were going to
52 avoid significant pH drift. We agree with the reviewer that this is a weakness of this current study
53 but we do acknowledge this in the manuscript and recommend a different approach for subsequent
54 studies. We respond to the rest of RC2's in turn below.

55 RC2: "I would love to see figure-S1 in the main body of the paper (with proper data legend), which
56 nicely compares the [B] vs pH relationship revealed here and previously in Mejía et al. (2013). Or
57 ternatively, I recommend to include the data by Mejía et al. (2013) in Figure 5B"

58 As mentioned in our response to RC1, we now include these data in Figure 5 of the revised
59 manuscript.

60 RC2: "Figure 5: It might be worthwhile to add horizontal error bars (uncertainties for the projected
61 11B values for borate due to the drifts in pH)."

62 This is a good idea, these are now added.

63 RC2: "In addition, I am curious if the authors considered more of a threshold-type response (e.g.,
64 step-wise increase) for the relationship between diatom B contents and seawater pH (Panel B),
65 rather than linear regression?"

66 This is an interesting point but given the uncertainties in both pH and [B] we would prefer not to
67 overly fit curves to the observed dataset. The statistics suggest a linear fit describes the data
68 adequately (albeit with some scatter) and such a two stepped relationship is not consistent with the
69 data from Mejia et al.

70 RC2: "Regarding the in-house TC460 standard used for validating the analytical methods. It was clear
71 to me that the variations in B contents in the TC460 shown in Figure 4C were due to supplemental
72 additions of different amounts of the NIST SRM951 reference material. But this appears not the case
73 for the variations in B contents shown in Figure 4A. Then, do they simply reflect the differences in
74 the amounts of TC460 dissolved?"

75 The variations in B content shown in Figure 4A reflect variations in the amount of boron loaded onto
76 the columns. We have attempted to make this clearer in the figure caption of this figure (line 471).

77 RC2: "I feel the manuscript will significantly benefit from having a short paragraph describing the
78 process of how diatoms produce their frustules, including how silicic acid is gained from seawater
79 into the cell and what happens afterwards (especially in the Silicate Deposition Vesicles: "SDV") to
80 deposit silica frustules. Perhaps, the paragraph should also have brief description of carbon
81 acquisition for photosynthesis (Line 364-371), to which an active intake of seawater borate is linked
82 (Line 364-372)."

83 These are good points and we have now added this 338-343 and 387-388.

84 RC2: "I have several questions and unclear points in the Section 3.2.2.... I think it is safe for authors to
85 acknowledge that assumption #1 is an entirely open question at this stage. Furthermore, I wonder
86 how assumption #2 is possible. I presume SDV plays central roles for frustule formation (silica
87 polymerization?). But it is mentioned that the internal pH of SDV should be around 5.5 (Line 334,
88 Line 347). At such pH, essentially all of dissolved B should exist as $B(OH)_3$, not $B(OH)_4^-$ (Fig. 6). How
89 can you incorporate something that does not exist?"

90 We now expand on the points raised here in the revised manuscript (lines 377-386).

91 In response to the other part of this comment – the SDV does play a very important role in the
92 formation of the opal frustule. This will be made clear in the revised manuscript.

93 The remainder of RC2's comments are minor and will be corrected in the revised manuscript.

94

1 **The pH dependency of the boron isotopic composition of diatom opal**
2 **(*Thalassiosira weissflogii*)**

3 Hannah K. Donald¹, Gavin L. Foster^{1,*}, Nico Fröhberg¹, George E. A. Swann², Alex J. Poulton^{3,4}, C. Mark
4 Moore¹ and Matthew P. Humphreys^{1,5}

5
6 ¹School of Ocean and Earth Science, National Oceanography Centre Southampton, University of
7 Southampton, Southampton, SO14 3ZH

8 ²School of Geography, University of Nottingham, University Park, Nottingham, NG7 2RD

9 ³Ocean Biogeochemistry and Ecosystems, National Oceanography Centre, Southampton, SO14 3ZH

10 ⁴The Lyell Centre, , Heriot-Watt University, Edinburgh, EH14 4AS

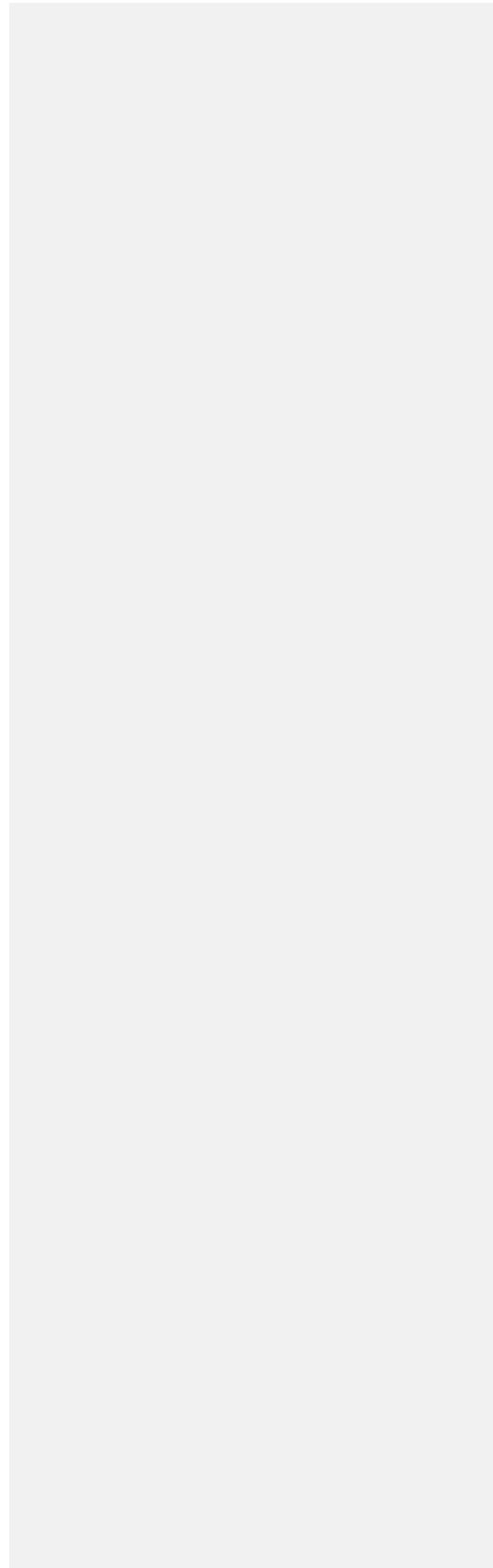
11 ⁵[School of Environmental Sciences, University of East Anglia, Norwich, NR4 7TJ](#)[NIOZ Royal Netherlands](#)
12 [Institute for Sea Research, Department of Ocean Systems \(OCS\), and Utrecht University, PO Box 59,](#)
13 [1790 AB Den Burg \(Texel\), the Netherlands](#)

14 *Corresponding Author

15
16 **Abstract**

17 The high latitude oceans are key areas of carbon and heat exchange between the atmosphere and the
18 ocean. As such, they are a focus of both modern oceanographic and palaeoclimate research. However,
19 most palaeoclimate proxies that could provide a long-term perspective are based on calcareous
20 organisms, such as foraminifera, that are scarce or entirely absent in deep-sea sediments south of
21 50°S latitude in the Southern Ocean and north of 40°N in the North Pacific. As a result, proxies need
22 to be developed for the opal-based organisms (e.g. diatoms) ~~that are~~ found at these high latitudes,
23 ~~and~~ which dominate the biogenic sediments ~~that are~~ recovered from these regions. Here we present
24 a method for the analysis of the boron (B) content and isotopic composition ($\delta^{11}\text{B}$) of diatom opal. We
25 ~~also~~ apply it for the first time to evaluate the relationship between seawater pH ~~and~~ $\delta^{11}\text{B}$ and B
26 concentration ([B]) in the frustules of the diatom *Thalassiosira weissflogii*, cultured ~~at~~ across a range
27 of [carbon dioxide partial pressure \(\$p\text{CO}_2\$ \)](#) and pH values. In agreement with existing data, we find
28 that the [B] of the cultured diatom frustules increases with increasing pH (Mejia et al., 2013). $\delta^{11}\text{B}$
29 shows a relatively well-defined negative trend with increasing pH, ~~a~~ completely distinct [relationship](#)
30 from any other biomineral previously measured. This relationship not only has implications for the
31 magnitude of the isotopic fractionation that occurs during boron incorporation into opal, but also
32 allows us to explore the potential of the boron-based proxies for palaeo-pH and palaeo- CO_2
33 reconstruction in high latitude marine sediments that have, up until now, eluded study due to the lack
34 of suitable carbonate material.

| 35
| 36



37 **1. Introduction**

38 The high latitude regions, such as the Southern Ocean and the subarctic North Pacific [Ocean](#), exert
39 key controls on atmospheric [carbon dioxide \(CO₂\)](#). Both areas are where upwelling of deep carbon-
40 and nutrient-rich water occurs, which promotes outgassing of previously stored carbon to the
41 atmosphere and nutrient fertilisation of primary productivity, in turn drawing down CO₂. The balance
42 of processes involved in determining whether these oceanic regions are a source or sink of CO₂ are
43 poorly understood, to the extent that the oceanic controls on glacial-interglacial pH and pCO₂ changes
44 remain a subject of vigorous debate (*e.g.* Martin, 1990; Sigman and Boyle, 2000). Recently, several
45 studies have shown how the boron isotope pH proxy applied to calcitic foraminifera successfully tracks
46 surface water CO₂ content, ~~and~~ thus document~~ing~~s changes in air-sea CO₂ flux along the margins of
47 these regions (*e.g.* Martínez-Botí et al., 2015; Gray et al. 2018). However, the lack of preserved marine
48 carbonates in areas that are thought to be key in terms of glacial-interglacial CO₂ change (*e.g.* the
49 polar Antarctic zone; Sigman et al., 2010) represents a currently insurmountable problem, ~~and~~
50 prevent~~ing~~s the determination of air-sea CO₂ flux using boron-based proxies in regions that are likely
51 to play the most important role in glacial-interglacial CO₂ change. There is therefore a clear need for
52 the boron isotope palaeo-pH proxy to be developed in biogenic silica (diatom frustules, radiolarian
53 shells), which is preserved in high-latitude settings, to better understand these key regions and their
54 role in natural climate change.

55
56 The boron isotopic system has been used extensively in marine carbonates for the reconstruction of
57 past ocean pH, and past atmospheric pCO₂ (*e.g.* Hemming and Hanson, 1992; Pearson and Palmer,
58 2000; Hönisch and Hemming, 2005; Foster, 2008; Henehan et al., 2013; Chalk et al. 2017; Sosdian et
59 al. 2018). Comprehensive calibration work has been completed for numerous species of foraminifera
60 that are currently used in palaeoceanographic reconstruction (*e.g.* Henehan et al. 2016; Rae et al.
61 2011). ~~From this, and~~ it has been shown that while $\delta^{11}\text{B}$ compositions are fairly similar among
62 carbonates, species-specific differences exist in the relationship between the [\$\delta^{11}\text{B}\$ boron isotopic](#)
63 [composition](#) of dissolved borate and ~~the $\delta^{11}\text{B}$ that~~ of foraminifera. Once this relationship is known, this
64 $\delta^{11}\text{B}$ -pH calibration can be applied to fossils found in deep-sea sediment cores, reliably reconstructing
65 past ocean pH and pCO₂ (*e.g.* Hönisch and Hemming, 2005; Foster, 2008, Hönisch et al., 2009; Chalk
66 et al., 2017). However, thus far the boron isotopic composition (expressed as $\delta^{11}\text{B}$) and B
67 concentration ([B]) of the siliceous fraction of deep-sea sediments remains poorly studied.

68
69 Early exploratory work by Ishikawa and Nakamura (1993) showed that biogenic silica and diatom ooze
70 collected from modern deep-sea sediments in the North and Equatorial Pacific had relatively high

71 boron contents (70-80 ppm), but a very light isotope ratio. For example, a diatom ooze was shown to
72 have a $\delta^{11}\text{B}$ of -1.1 ‰ whilst radiolarian shells had a $\delta^{11}\text{B}$ of +4.5 ‰. While some of this light $\delta^{11}\text{B}$ may
73 have partly arisen due to clay contamination (reducing the diatom ooze sample by up to 3 ‰; Ishikawa
74 and Nakamura, 1993) it also likely reflects an opal:seawater isotopic fractionation arising from the
75 substitution of borate for silicate in tetrahedral sites in the opal (Ishikawa and Nakamura, 1993). A
76 similarly light $\delta^{11}\text{B}$ was also observed in marine cherts from deep sea sediments by Kolodny and
77 Chaussidon (2004; -9.3 to +8 ‰), but these are likely diagenetic and therefore are unlikely to be
78 primary seawater precipitates. A recent culture study of the diatoms *Thalassiosira weissflogii* and *T.*
79 *pseudonana* showed that the boron content of cultured opal was significantly lower than suggested
80 by the bulk sampling of Ishikawa and Nakamura (1993) at around 5-10 ppm, increasing as pH increased
81 from 7.6 to 8.7 (Mejia et al., 2013; ~~Supplementary Figure S1~~). This suggests seawater
82 tetrahydroxyborate anion (borate; $\text{B}(\text{OH})_4^-$) is predominantly incorporated into the diatom frustule
83 rather than boric acid ($\text{B}(\text{OH})_3$); and implies there is potential for the boron content of diatom opal to
84 trace pH in the past (Mejia et al., 2013).

85
86 Here, the relationship between $\delta^{11}\text{B}$ of the frustules of the diatom *T. weissflogii* and seawater pH is
87 investigated for the first time using a batch culturing technique and different air- CO_2 mixtures to
88 explore a range of pH (8.54 ± 0.57 to 7.48 ± 0.06). The aim of this study was also to develop a
89 methodology for measuring the boron isotopic composition of biogenic silica by MC-ICP-MS and apply
90 this method to explore the response of the boron-based proxies ([B] and $\delta^{11}\text{B}$) in diatom frustules to
91 changing pH. Ultimately, we show how boron isotopes measured in diatom frustules may provide
92 further insight into boron uptake and physiological activity within diatoms; and ~~we~~ test the potential
93 of $\delta^{11}\text{B}$ and boron content in diatoms as proxies for the ocean carbonate system.

94

95 2. Methods

96 2.1 Experimental Set up

97 The centric diatom *T. weissflogii* (Grunow in van Heurck, PCC 541, CCAP 1085/1; Hasle and Fryxell,
98 1977) was grown in triplicate in ~~K/1~~-enriched sterile and filtered seawater (K/1; 0.2 μM ; seawater
99 sourced from Labrador Sea; Keller et al., 1987) in 3 L glass Erlenmeyer flasks for a maximum of one
100 week for each experiment. Initial nutrient concentrations within the seawater before enrichment
101 were assessed on a SEAL Analytical QuAAtro analyser with a UV/vis spectrometer and ranged from
102 23.3 to 27.5 μM for nitrate(+nitrite), 4.3 to 5.4 μM for silicic acid, and 1.4 to 1.6 μM for phosphate.
103 The culture experiments were bubbled with air- CO_2 mixtures in different concentrations (sourced
104 from BOC; www.boconline.co.uk) to provide a pH range at constant bubble rates, ~~and with~~ every flask

105 was agitated by hand twice daily to limit algal settling and aggregation. The monocultures were grown
106 in nutrient replete conditions at constant temperature (20°C) and on a 12h:12 h light:dark cycle (with
107 $192 \mu\text{E m}^{-2} \text{s}^{-1}$, or $8.3 \text{ E m}^{-2} \text{d}^{-1}$ during the photoperiod). The diatoms were acclimated to each $p\text{CO}_2$
108 treatment for at least 10 generations before inoculating the culture experiment flasks. All culture
109 handling was completed within a laminar flow hood to ensure sterility. The flow hood surfaces were
110 cleaned with 90% ethanol before and after handling, as well as the outer surface of all autoclaved
111 labware entering the laminar flow hood such as bottles and pipettes.

112
113 The cultured diatom samples were collected by centrifugation at 96 h, during the exponential growth
114 phase. Each flask was simultaneously disconnected from the gas supply, ~~and-with~~ the culture ~~was~~
115 immediately centrifuged at 3700 rpm for 30 minutes into a pellet, rinsed with MilliQ, and frozen at -
116 20°C in sterile plastic 50 mL centrifuge tubes. Around 10 mg of diatom biomass was harvested in each
117 experiment.

118
119 **2.2. Growth rate and cell size**
120 A 5 mL sub-sample was taken from each culture flask through sterilised Nalgene tubing into sterile
121 syringes, and sealed in sterile 15 mL centrifuge tubes. Triplicate cell counts using a Coulter
122 Multizier^{TM3} (Beckman Coulter) were performed daily on each experimental flask. Growth rates were
123 calculated using equation 1:

124
$$\mu = (\ln N_t - \ln N_i) / (t - t_i) \quad (1)$$

125 ~~Where-where~~ N_i is the initial cell density at the start of the experiment (t_i) and N_t is the cell density at
126 time t . Triplicate estimates of cell size were also determined using the Coulter Multizier^{TM3}, to
127 determine the mean cell size over time in each flask. Figure 1 shows that although there is no
128 statistically significant relationship between pH and diatom growth rate, cell size does show a small,
129 but statistically significant, positive slope.

130 **2.3 pH, DIC and $\delta^{11}\text{B}$ of the culture media**
131 A pH meter (Orion 410A) calibrated using standard National Bureau of Standards (NBS) buffers prior
132 to sample extraction was used to monitor the evolution of pH through the experiment on a daily
133 basis. For fully quantitative constraints on the carbonate system of the culture media, dissolved
134 inorganic carbon, DIC was measured in triplicate, every other day, for each pH treatment (*i.e.* once
135 per experiment flask). The 100 mL sample bottles were filled to overflowing and immediately closed

136 with ground glass stoppers, then uncapped to be poisoned with ~~1 mL~~ 20 μ L saturated mercuric
137 chloride solution (HgCl₂) to prevent any further biologically-induced changes in DIC, ~~and before being~~
138 ~~stored~~ sealed with a 1 mL air headspace and Apiezon L grease, and stored in complete darkness until
139 analysis (Dickson et al., 2007). Analysis of DIC was performed by acidification with excess 10%
140 phosphoric acid and CO₂ transfer in a nitrogen gas stream to an infrared detector using a DIC
141 Analyzer AS-C3 (Apollo SciTech, DE, USA) at the University of Southampton. The DIC results were
142 calibrated using measurements of batch 151 certified reference material obtained from A. G.
143 Dickson (Scripps Institution of Oceanography, CA, USA). The accuracy of the DIC analysis was ca. 3
144 μ mol kg⁻¹. Carbonate system parameters, including seawater pCO₂, were calculated using measured
145 pH_{NBS} and DIC values, temperature, salinity and nutrients with the CO₂SYS v1.1 program (van
146 Heuven et al., 2011; using constants from Dickson, 1990; Lueker et al., 2000; Lee et al., 2010), which
147 was also used to convert pH meter readings from the NBS to the Total scale (used throughout).

148 All flasks were initially filled with media from the same large batch, and all culture treatments
149 therefore started with the same initial pH. The pH for all treatments was then altered by bubbling
150 through the different air-CO₂ mixtures, ranging from low pH (target = 1600 ppm, high pCO₂) to high
151 pH (target = 200 ppm, low pCO₂). Almost all treatments held relatively constant DIC and pH until the
152 final 24 hours of the experiment, when marked changes in DIC and pH in all culture treatments were
153 observed (Figure 2), which in most cases was likely due to the growth of diatoms and an associated
154 net removal of DIC, despite the constant addition of pCO₂. In order to account for these non-steady
155 state conditions of the carbonate system, the mean pH and pCO₂ of each treatment were calculated
156 based on the number of cells grown per 24 hours along with the pH/pCO₂ measured in that 24 hours,
157 thus adjusting for the observed exponential growth rate of *T. weissflogii* (Table 1).

158
159 The boron concentration of the culture media was not determined but is assumed to be the same as
160 Labrador seawater (~4.5 ppm; Lee et al., 2010). The boron isotopic composition of the culture media
161 was determined using standard approaches (Foster et al., 2010) to be 38.8 ± 0.19 ‰ (2 s.d.).

162 2.4 Preparing cultured diatoms for $\delta^{11}\text{B}$ and B/Si analysis

163 In order to examine reproducibility and accuracy of our boron measurements, an in-house diatom
164 reference material was used to develop a method for measuring boron isotopes and boron
165 concentration in biogenic silica. A British Antarctic Survey core catcher sample (TC460) from core
166 TC460 in the Southern Ocean (-60.81534° N, -50.9851° E, water depth 2594 m) was used for this
167 purpose (supplied by C.-D. Hildebrand [British Antarctic Survey]). Although the diatom assemblage
168 was not characterised in the core catcher, the nearest sediment sample in the core is dominated by

169 *Hyalochaete Chaetoceros* resting spores, representing circa 70% of the total diatom content, with sea
170 ice and cool open water species making up the bulk of the remaining 30% (e.g. *Actinocyclus*
171 *actinochilus*, *Fragilariopsis curta*, *F. cylindrus*, *F. obliquecostata*, *Odontella weissflogii*, *Thalassiosira*
172 *antarctica*). A pure diatom sample of mixed species was separated from this bulk sediment and
173 cleaned of clay contamination at the University of Nottingham following an established diatom
174 separation technique (Swann et al., 2013). Briefly, the bulk sample underwent organic removal and
175 carbonate dissolution (using 30% H₂O₂ and 5% HCl), heavy liquid separation in several steps at
176 different specific gravities using sodium polytungstate (SPT), and visual monitoring throughout the
177 process to ensure the sample was free from non-diatom material, such as clay particulates. After the
178 final SPT separation, samples were rinsed thoroughly with MilliQ and sieved at 10 µm to remove all
179 SPT traces.

180

181 The culture samples and the diatom fraction from TC460 were first acidified (H₂SO₄) and organics
182 were oxidised using potassium permanganate and oxalic acid (following Horn et al., 2011 and Mejía
183 et al., 2013). The samples were rinsed thoroughly using MilliQ water via centrifugation and transferred
184 to acid-cleaned Teflon beakers. A secondary oxidation was completed under heat using perchloric
185 acid. Finally, the organic-free samples were rinsed thoroughly with MilliQ via filtration.

186

187 In the boron-free HEPA filtered clean laboratory at the University of Southampton, each sample was
188 dissolved completely in a gravimetrically known amount of NaOH (0.5 M from 10 M concentrated
189 stock supplied by Fluka) at 140°C for 6 to 12 h, and briefly centrifuged prior to boron separation to
190 ensure no insoluble particles were loaded onto the boron column. Anion exchange columns containing
191 Amberlite IRA 743 resin were then used to separate the matrix from the boron fraction of each sample
192 following Foster (2008). Briefly, the dissolved opal was loaded directly onto the column without
193 buffering and the matrix removed with 9 x 200 µL washes of MilliQ. This was collected for subsequent
194 analysis and the pure boron fraction was then eluted and collected in 550 µL of 0.5 M HNO₃ acid. The
195 level of potential contamination was frequently monitored using total procedural blanks (TPB)
196 measured in every batch of columns. The TPB comprised an equivalent volume of sodium hydroxide
197 (NaOH, 0.5 M) as used in the samples of each batch (ca. 0.2 - 4 mL). This was analysed following the
198 sample analysis protocols detailed below, and typically the TPBs for this work contained less than 40
199 pg of boron. This equates to a typical blank contribution of ca. 0.015%, which results in a negligible
200 correction and is therefore ignored here.

201

202 Prior to isotope analysis, all boron fractions were collected in pre-weighed acid cleaned Teflon beakers
203 and their mass was recorded using a Precisa balance. A 10 µL aliquot was taken and diluted with 490
204 µL 0.5 M HNO₃ in acid cleaned plastic centrifuge tubes (2 mL). This was then analysed using a Thermo
205 Fisher Scientific Element 2XR ICP-MS at the University of Southampton, with boron concentration
206 determined using standard approaches and a gravimetric standard containing boron, silicon, sodium,
207 and aluminium. In order to determine the B/Si ratio, and hence the B concentration of the opal, the
208 Si concentration must also be quantitatively measured. This is achieved here by using a known
209 concentration and mass of NaOH to dissolve each sample, and by measuring the Si/Na ratio the Si
210 concentration of each opal sample can be determined. From this, assuming a chemical formula of
211 SiO₂.H₂O and a H₂O content of 8% (Hendry and Anderson, 2013), the B content of the opal in ppm can
212 be estimated. As detailed above, during the purification procedure, sample matrix was washed off
213 the column using MilliQ, and collected in pre-weighed acid cleaned Teflon beakers. These samples
214 were then diluted with 3 % HNO₃ enriched with Be, In and Re for the internal standardisation and
215 measured on the Thermo Scientific X-series ICP-MS. The standards run on the X-Series consisted of
216 varied concentrations of the gravimetric standard also used on the Element, containing B, Si, Na and
217 Al.

218
219 The boron isotopic composition of the biogenic silica samples was determined on a Thermo Scientific
220 Neptune MC-ICP-MS, also situated in a boron-free HEPA filtered laboratory at the University of
221 Southampton, following Foster (2008). Instrument induced fractionation of the ¹¹B/¹⁰B ratio was
222 corrected using a sample-standard bracketing routine with NIST SRM 951, following Foster (2008).
223 This allows a direct determination of δ¹¹B without recourse to an absolute value for NIST SRM 951
224 (Foster, 2008) using the following equation, where ¹¹B/¹⁰B_{standard} is the mean ¹¹B/¹⁰B ratio of the
225 standards bracketing the sample of interest.

226
227
$$\delta^{11}\text{B} = \left[\left(\frac{{}^{11}\text{B}/{}^{10}\text{B}_{\text{sample}}}{{}^{11}\text{B}/{}^{10}\text{B}_{\text{standard}}} \right) - 1 \right] \times 1000 \quad (2)$$

228
229 The reported δ¹¹B is an average of the two analyses, with each representing a fully independent
230 measurement (*i.e.* the two measurements did not share blanks or bracketing standards). Machine
231 stability and accuracy was monitored throughout the analytical session using repeats of NIST SRM 951,
232 as well as boric acid reference materials AE120, AE121 and AE122 that gave δ¹¹B (± 2 s.d.) of -20.19 ±
233 0.20 ‰, 19.60 ± 0.28 ‰, and 39.31 ± 0.28 ‰, that are within error of the gravimetric values from Vogl
234 and Rosner (2012).

235

236 The ~~reproducibility~~ ~~reproducibilities~~ of the $\delta^{11}\text{B}$ and [B] measurements were assessed by repeat
237 measurements of TC460 of different total B concentration (11 to 34 ng of B). In order to assess the
238 accuracy of this method, we follow Tipper et al. (2008) and Ni et al. (2010) and use standard addition.
239 To this end, known amounts of NIST SRM 951 standard were mixed with known quantities of TC460.
240 All mixtures were passed through the entire separation and analytical procedure, including aliquots
241 of pure standard and sample. A sodium acetate - acetic acid buffer was added to all 951 boric acid
242 used prior to mixing, to ensure the pH was sufficiently elevated for the column separation procedure
243 (following Foster, 2008). The amount of biogenic silica matrix added to the columns for each mixture
244 was kept constant, so the volume added to the column was altered for each mixture accordingly.
245 Uncertainty in the $\delta^{11}\text{B}$ calculated for each mixture was determined using a Monte Carlo procedure (n
246 = 1000) in R (R Core Team, 2019) propagating uncertainties, at 95% confidence, in known isotopes
247 ratios ($\pm 0.2\text{‰}$), sample concentration ($\pm 6\%$), and measured masses ($\pm 0.5\%$).
248

249 3. Results and Discussion

250 3.1 Analytical Technique

251 3.1.1. Purification

252 The Na, Si_i and Al concentrations of the matrix fraction of several replicates of the diatom fraction of
253 TC460 are shown in Figure 3a-d. Prior to purification, Na and Si concentrations were consistently
254 around 265 and 114 ppm respectively, whereas Al was more variable at 5-25 ppb. The boron content
255 of these matrix samples in all cases was at blank level. -The concentration of these elements in the
256 boron fraction is shown in Figure 3e-g, highlighting that the column procedure ~~is~~ ~~was~~ sufficient to
257 concentrate boron and remove Na and Si_i which are both present at sub-5 ppb level (*i.e.* at less than
258 0.002 % of matrix concentration). The Al is likely present in the diatom frustule (*e.g.* Koning et al.,
259 2007) and is elevated in the boron fraction compared to the matrix fraction (Figure 3). Diatom-bound
260 Al is likely present as the anion $\text{Al}(\text{OH})_4^-$, hence its elevation in the boron fraction. Although this is a
261 detectable level of Al, it is unlikely that this level of contamination will influence the mass fractionation
262 of these samples when measured by MC-ICP-MS (Foster, 2008; Guerrot et al., 2010).
263

264 3.1.2. Accuracy and Reproducibility

265 Throughout the duration of this study, a single dissolution of the diatom fraction of TC460 was
266 measured 18 times in separate analyses at various concentrations, in order to assess external
267 reproducibility of this method. Carbonates generally have a reproducibility of $\pm 0.20\text{‰}$ (2σ) at an
268 analyte concentration of 50 ppb boron using the MC-ICP-MS methods at [the University of](#)
269 Southampton (*e.g.* Chalk et al., 2017). The repeated measurements of TC460 gave a reproducibility of

270 $\pm 0.28 \text{ ‰}$ (2σ) over 18 samples, ranging from 19 ppb to 61 ppb (11 to 34 ng) boron (Figure 4). The
271 ~~similar insensitivity of $\delta^{11}\text{B}$ regardless of the~~ boron concentration analysed confirms that blank
272 contamination during purification is not significant. Figure 4 shows that there is also no correlation
273 between Al content of the boron fraction and measured $\delta^{11}\text{B}$, confirming ~~that~~ Al contamination does
274 not influence mass fractionation.

275
276 Figure 4 shows the results of the standard addition experiment, and when the uncertainty in the $\delta^{11}\text{B}$
277 of the mixture is considered, it is clear that nearly all the mixtures lie within error of the 1:1 line,
278 indicating that there is a lack of a significant matrix effect when analysing the $\delta^{11}\text{B}$ of biogenic silica as
279 described herein. A least-squares linear regression of the mixtures has a slope of 1.01 ± 0.07 and an
280 intercept of $-0.15 \pm 0.29 \text{ ‰}$, implying the approach is accurate to $\pm 0.29 \text{ ‰}$, which is remarkably similar
281 to the stated reproducibility of TC460 ($\pm 0.28 \text{ ‰}$ at 2σ).

282

283 B and Si content were determined separately and combined post-analysis in order to estimate the
284 B/Si ratio for each sample and hence the B concentration. The reproducibility of this method was
285 tested using six repeats of the diatom fraction of TC460. The mean of all six measurements is $2.99 \pm$
286 0.64 ppm ; (2σ ; Figure 4), implying this multi-stage method of determining the B content of diatoms is
287 precise to $\pm 20 \text{ ‰}$ at 95% confidence.

288

289 3.2. Diatom Cultures

290 3.2.1. Boron content of the frustule of *T. weissflogii*

291 The boron content of *T. weissflogii* increases as a function of pH from around $\sim 1 \text{ ppm}$ to $\sim 4 \text{ ppm}$ over
292 a range of average culture pH from 7.5 to 8.6 (Figure 5; Table 2). While this is lower by an order of
293 magnitude than the limited previous studies of boron in sedimentary diatoms (Ishikawa and
294 Nakamura, 1993), it is similar to boron concentration in the bulk diatom fraction of TC460 (Figure 4D5)
295 and to that observed in previous culturing studies of this diatom species (Figure 5; Meija et al., 2013).
296 In detail, however, our concentrations are around 2-3 times lower than Meija et al. (2013), perhaps
297 due to: (i) the different analytical methods used (laser ablation ICP-MS vs. solution here); (ii) ~~Figure~~
298 ~~A1) differences in cleaning methods; and/or (iii) differences in culturing methodology.~~ -Despite the
299 scatter between ~~our~~ treatments (also seen in Meija et al., 2013; Figure 5; ~~Figure A1~~), a least squares
300 regression through the treatments is significant at the 95% confidence level ($y = 2.15x - 15.56$, $R^2 =$
301 0.46 , $p = 0.015$; Figure 5). The cause of this scatter between treatments is not known but a likely
302 contributor is the relatively high variability in the carbonate system which was observed in each
303 treatment due to the growth of the diatoms in this batch culture setup (Figure 2).

Formatted: Highlight

304
305 Boron is an essential nutrient for diatoms (Lewin, 1966) and it is likely that boric acid passively diffuses
306 across the cell wall to ensure the diatom cell has sufficient boron to meet its biological needs.
307 However, if boric acid were the sole source of boron for the diatoms measured here we might expect
308 a decrease in boron content as pH increases and external dissolved boric acid concentration declines
309 (Figure 6).

310
311 Several studies note that a number of higher plants have mechanisms for also actively taking up boron,
312 leading to large variations in internal boron concentrations (Pfeffer et al., 2001; Dordas and Brown,
313 2000; Brown et al., 2002). Indeed, on the basis of a similar dataset to that collected here, Meija et al.
314 (2013) suggested that borate is likely transported across the cell wall of *T. weissflogii* as some function
315 of external borate concentration, which shows a positive relationship with external pH (Figure 6). This
316 hypothesis is developed and discussed further in the next section.

317
318 **3.2.2. Frustule $\delta^{11}\text{B}$ of *T. weissflogii***
319 The $\delta^{11}\text{B}$ of *T. weissflogii* are isotopically light compared to seawater (39.6 ‰; Foster et al., 2010), with
320 an average value across all treatments of -3.95 ‰ (Table 2). Despite the scatter between treatments,
321 similar to the [B] data, Figure 55 shows that there is a clear relationship between the $\delta^{11}\text{B}$ of the diatom
322 frustule and pH ($R^2 = 0.463$, $p < 0.01$), albeit with a negative and relatively shallow slope ($y = -2.6137x$
323 $+ 17.12534$).

324
325 These results confirm that biogenic silica, free from clay contamination, has a very light boron isotopic
326 composition (Ishikawa and Nakamura, 1993). However, the observed relationship between $\delta^{11}\text{B}$ in *T.*
327 *weissflogii* and pH is radically different to that which is observed in carbonates (Figure 55), implying a
328 distinctive incorporation mechanism for boron into diatom opal. Much work has been carried out in
329 recent years to show that boron is incorporated in carbonates predominantly as the borate ion with
330 minor, if any, isotopic fractionation (e.g. see Branson, 2018 for a review). It is similarly thought that
331 the borate ion is incorporated into opal in an analogous fashion to its incorporation into clays
332 (Ishikawa and Nakamura, 1993; Kolodny and Chaussidon, 2004). However, such a mechanism in
333 isolation would only be able to generate $\delta^{11}\text{B}$ in opal of ~13 ‰ (at the lowest pH). Given the
334 preponderance of isotopically light diatoms, radiolaria and chert $\delta^{11}\text{B}$ in the literature (including this
335 study; Kolodny and Chaussidon, 2004; Ishikawa and Nakamura, 1993), it is therefore likely that there
336 is an additional light isotopic fractionation of boron on its incorporation into opal, although its
337 absolute magnitude is currently unknown (Kolodny and Chaussidon, 2004).

338

339 To make their frustules out of biogenic silica, aqueous $\text{Si}(\text{OH})_4$ is taken up by the diatom cell via active
340 transport by silicon transporter proteins (Amo and Brzezinski, 1999). Once $\text{Si}(\text{OH})_4$ has entered the
341 cell, it accumulates in vacuoles that tend to have a high pH in order to prevent polycondensation of
342 $\text{Si}(\text{OH})_4$ at its higher concentration in the vacuole (Vrieling et al., 1999). The accumulated $\text{Si}(\text{OH})_4$ is
343 then transported to the silicon deposition vesicle (SDV), which is an acidic compartment where the
344 formation of biogenic silica and the construction of the frustule occurs. -Without knowledge of the
345 isotopic fractionation of boron on incorporation into biogenic silica, the interpretation of our new $\delta^{11}\text{B}$
346 data is ~~therefore~~ challenging. This difficulty is further increased given that the fluid in the ~~silica~~
347 ~~deposition vesicle (SDV) in diatoms~~ is unlikely to have the ~~boron isotopic composition of same $\delta^{11}\text{B}$ as~~
348 external seawater, and ~~is likely at a~~ relatively acidic pH (~5.5; Meija et al., 2013; Vrieling et al., 1999)
349 ~~is likely~~ to promote polymerisation of $\text{Si}(\text{OH})_4$. Nonetheless, the broad similarity between the $\delta^{11}\text{B}$ of
350 our cultured *T. weissflogii* with the bulk diatom fraction measured here from sample TC460, and the
351 bulk diatom fraction and radiolarian skeleton measured by Ishikawa and Nakamura (1993), suggests
352 ~~that~~ a large part of the light isotopic composition of biogenic silica is driven by the isotopic
353 fractionation on incorporation rather than “vital effects” relating to the $\delta^{11}\text{B}$ and pH of the SDV in the
354 different species and organisms. That being said, the >3‰ range between different pH treatments in
355 *T. weissflogii* and the >10 ‰ difference between our *Chaetoceros* dominated bulk diatom fraction
356 from TC460 and the cultured *T. weissflogii*, as well as the negative relationship between pH and
357 diatom $\delta^{11}\text{B}$ (Figure 5), argues against a simple two-step model involving ~~the incorporation of seawater~~
358 borate ion ~~incorporation from seawater with and~~ a fixed isotopic fractionation ~~on incorporation~~.

359

360 The $\delta^{11}\text{B}$ of the fluid from which our *T. weissflogii* precipitated their frustules can be calculated if
361 we assume the pH in the SDV of our *T. weissflogii* is 5.5 across all our treatments (Meija et al.,
362 2013). ~~Given that at this pH the $\delta^{11}\text{B}$ of borate is ~13 ‰, This suggests that the~~ isotopic
363 composition of this fluid is lighter than seawater, even if we assume an arbitrary ~~-~~10 ‰ isotopic
364 fractionation on incorporation (blue circles in Figure 7a). Furthermore, the $\delta^{11}\text{B}$ of the SDV fluid
365 is inversely correlated with the $\delta^{11}\text{B}$ of either dissolved borate or dissolved boric acid (Figure 7a).

366 As discussed above ~~and illustrated schematically in Figure 8~~, Meija et al. (2013) suggested that
367 there are two sources of boron in a diatom cell: (i) passively diffused and isotopically heavy boric
368 acid; and (ii) actively ~~incorporated-transported~~ isotopically light borate ion (see Figure 86).

369 Assuming that: (a) no additional fractionation occurs during uptake and diffusion; and (b) only the
370 borate ion is incorporated into the frustule, we can calculate the relative contribution of these

Formatted: Subscript

Formatted: Not Highlight

Formatted: Subscript

Formatted: Subscript

Formatted: Subscript

Formatted: Not Highlight

371 two sources of boron as a function of external pH (Figure 7b). This treatment shows that the
372 relative concentration of borate derived boron in the SDV fluid increases as external pH increases,
373 though the absolute values here are a function of the magnitude of the isotopic fractionation on
374 incorporation, ~~and~~ so we only have confidence in the trends shown in Figure 7b. Nonetheless,
375 given that ~~the~~ dissolved boric acid concentration decreases and dissolved borate increases as pH
376 is increased (Figure 6), this is perhaps not surprising.

377 ~~While~~ ~~this finding is also~~ entirely compatible with the trend of increasing boron content of *T.*
378 *weissflogii* observed as pH increases (Figure 5), ~~an added complication is that at pH ~5.5 the~~
379 ~~concentration of borate ion in the SDV is likely to be relatively low (Figure 6).~~ ~~However, the~~
380 ~~timescales required~~ ~~however~~ to reach equilibrium in the boron system are short (e.g. around 95
381 μ s; Zeebe et al., 2001), meaning that ~~once any aqueous borate had been~~ incorporated into the
382 frustule ~~there would be a continuous supply replenishing concentrations immediately replenished~~
383 ~~to its equilibrium values from the ready by conversion of~~ the more ~~dominant abundant~~ boric
384 acid. Although relevant partition coefficients are likely to be different, a similar process ensures
385 ~~the quantitative removal of boron from pH <7 solutions by the Amberlite 743 anion exchange~~
386 ~~resin used for boron purification prior to analysis by MC-ICPMS (see above; Lemarchand et al.,~~
387 ~~2002).~~

388 ~~Active bicarbonate ion uptake accounts for a substantial amount of the carbon fixed by phytoplankton~~
389 ~~(e.g. Tortell et al., 2006).~~ ~~As a result,~~ Mejía et al. (2013) proposed that the enrichment of borate ion
390 into the SDV of *T. weissflogii* and *T. pseudonana* was the result of the active co-transport of borate ion
391 with bicarbonate ion by bicarbonate transporter proteins. Borate is transported because of its similar
392 charge and size to HCO_3^- and the phylogenetic similarity between bicarbonate and borate transporters
393 (Mejía et al., 2013). In ~~this our~~ model, as external borate ion concentration increases, the borate leak
394 into the diatom cell is also increased. An additional factor is ~~the~~ HCO_3^- transport, which may be
395 proportionally up-regulated as external CO_2 content decreases (~~as and~~ external pH increases) in order
396 to provide the diatom cell with sufficient carbon (Mejía et al., 2013). This may therefore offer ~~a~~
397 ~~additional factor~~ ~~way of~~ driving an elevation of the borate content of the SDV as pH increases (Mejía
398 et al., 2013). Regardless of the exact mechanism, ~~a~~ SDV fluid ~~that displays a boron isotopic~~
399 ~~composition as an inverse function of~~ ~~with an inverse relationship between $\delta^{11}\text{B}$ and~~ pH is required to
400 explain the ~~observed $\delta^{11}\text{B}$ composition~~ of the ~~frustule of~~ *T. weissflogii* ~~frustule~~ measured here. A
401 simple model whereby external borate ion is an increasingly important contributor to the boron in the
402 SDV as pH increases is able to explain the observed dependency of boron content and $\delta^{11}\text{B}$ on pH.

403 However, a more complete model of the boron systematics in diatom opal requires a better
404 understanding of ~~the~~ isotopic fractionations on incorporation of boron into biogenic silica, the
405 environmental controls on this fractionation, and the nature of the partitioning of ~~the~~ boron within
406 the diatom cell and into biogenic silica.

408 3.2.3. Boron-based pH proxies in diatom opal

409 The $\delta^{11}\text{B}$ -pH and B-pH relationships derived here for *T. weissflogii* potentially offer two independent
410 means to reconstruct the past pH of seawater, particularly in those regions key for CO_2 and heat
411 exchange where foraminifera are largely absent (e.g. ~~at the high~~ ~~Southern and Northern~~ latitudes).
412 However, the current calibrations (Figure 5) are relatively uncertain, ~~and this~~ which may preclude their
413 application to some situations. For instance, recasting the $\delta^{11}\text{B}$ -pH relationship in terms of $\delta^{11}\text{B}$ as the
414 dependent variable and using a regression method that accounts for uncertainty in X and Y variables
415 (SIMEX; Carroll et al., 1996) gives the calculated residual pH of the regression as ± 0.28 pH units. For
416 the [B] vs. pH relationship, this uncertainty is ± 0.36 pH units. At ~~TA or DIC typically found in the~~ typical
417 surface ocean conditions, such a variability in pH would translate to ~~estimated~~ seawater $p\text{CO}_2$
418 variability of up to ca. ± 250 ppm. Although encouraging, this treatment suggests that additional work
419 is needed before the relationship between $\delta^{11}\text{B}$ and boron content of diatom opal and seawater pH is
420 a sufficiently precise proxy for a fully quantitative past ocean pH. In particular, future culturing efforts
421 should aim to more carefully control the pH of the culture media. This could be achieved by either
422 using larger volume dilute batch cultures, ~~and/or~~ by harvesting the diatoms earlier in the experiment
423 prior to any significant drift in the carbonate system, ~~and/or~~ ~~more robustly through~~ by using a more
424 robust steady-state chemostat method (e.g. Leonardos and Geider, 2005).

426 4. Conclusions

427 In the first study of its kind, ~~using we use~~ a modified version of the carbonate boron purification
428 technique of Foster (2008), ~~we to~~ show that the $\delta^{11}\text{B}$ of *T. weissflogii* opal is pH sensitive but
429 isotopically light (-3.95 ‰ on average), and has an inverse relationship with external seawater pH.
430 Using a novel ICP-MS method we also show that the boron content of *T. weissflogii* opal ~~increased~~
431 increases with increasing pH, supporting the only other study investigating boron in diatoms (Mejía et
432 al., 2013). This suggests that more borate is incorporated into the diatom frustule as the dissolved
433 borate abundance increases with external pH. A simple model is presented, based on Mejía et al.
434 (2013), which implies both of these findings could be due to ~~there being two distinct sources of the~~
435 boron in the SDV ~~having two distinct sources~~: external boric acid and external borate ion, with the
436 balance of each source changing with external pH. While these results are encouraging, ~~and~~

Formatted: Font: Italic

437 ~~suggest~~suggesting that the boron proxies in diatom opal may hold considerable promise as a tracer of
438 past ocean pH, more work is needed to fully understand the boron systematics of diatom opal. In
439 particular, there is an urgent need to place boron in opal on a firmer grounding with precipitation
440 experiments in the laboratory at controlled pH to determine the magnitude of boron isotopic
441 fractionation on boron incorporation into opal ~~as well as, and subsequently~~ the dependence of this
442 fractionation on other environmental factors.

443

444 **Acknowledgements**

445 We wish to thank Claus-Dieter Hildebrand for supplying the diatom-rich sediment sample TC460. John
446 Gittins, Mark Stinchcombe, Chris Daniels and Lucie ~~Munns-Daniels~~ are acknowledged for their help
447 during the culturing and subsequent nutrient and carbonate system analysis. ~~Heather~~ Heather Stoll is also
448 thanked for her useful discussions on this topic. Financial support for this study was provided by the
449 Natural Environmental Research Council (UK) to H.K.D. (grant number 1362080) and to G.L.F.
450 (NE/J021075/1).

451

452

453

454

455

456

457

458

459

460 **Figure Captions**

461 **Figure 1.** Diatom growth rate and cell size as a function of pH labelled according to CO₂ treatment.
462 Linear least squares regressions, including R² and p-values are also shown.

463 **Figure 2:** Each culture treatment labelled according to target pCO₂ and showing the evolution in
464 the culture media through the experiment. All treatments exhibit changes in DIC due to diatom
465 growth balanced with the input of pCO₂. The higher pCO₂, the more DIC increases towards the
466 end of the experiment.

467 **Figure 3:** (a-d) Concentration of Na, Si, Al and B in the Matrix Fraction by ICP-MS. These analyses
468 suggest blank levels of B are present in the matrix washed off the Amberlite IRA 743 resin-based
469 column. (e-f) Concentration of the Na, Si and Al in the boron fraction indicating blank levels of Na
470 (ca. 1.7 ppb) and Si (ca. 1.9 ppb); and a higher concentration of Al (ca. 68 ppb) are present.

471 **Figure 4:** (A) The reproducibility of the TC460 diatom core catcher in-house standard. ~~This shows all~~
472 ~~samples of different concentration (~10 to ~30 ng B) lie within error of the mean (5.98 ‰ ± 0.28 ‰,~~
473 ~~2σ) at varied concentrations.~~ This compares well to carbonates (2σ = 0.20 ‰). (B) Aluminium
474 concentration of the B fraction from TC460 (as ppb of the solution analysed for δ¹¹B) shows no
475 correlation with δ¹¹B, likely suggesting there is no significant effect on mass fractionation for this
476 level of Al. (C) The results of the standard addition experiment. The blue line is a least squares
477 regression between the measured δ¹¹B of each mixture (green circles) and the calculated δ¹¹B of that
478 mixture given known end-member values (end members shown as blue circles). R² = 0.97, p < 0.0001,
479 slope = 1.01 ± 0.07 and intercept = -0.15 ± 0.29. 1:1 line is shown as a black line and dotted blue lines
480 show the 95% confidence limit of the regression. Note that the end members were not used in the
481 regression. (D) B content in ppm of six repeat samples of the diatom fraction of TC460. The black line
482 indicates the mean value; and the grey lines show 2σ, of 2.99 ± 0.64 ppm.

483 **Figure 5:** ~~(A) (A)~~ δ¹¹B of *T. weissflogii* diatom opal plotted against aqueous borate, labelled according
484 to pCO₂ treatment. Also shown are published deep sea coral *Desmophyllum dianthus* (Anagnostou
485 et al., 2012) and foraminifera δ¹¹B (*Globigerinoides ruber* and *Orbulina universa*; Henehan et al.,
486 2013; Henehan et al., 2016, respectively). Least squares regression lines are also shown. Error bars
487 on δ¹¹B borate are shown at 95% level of confidence and relate to the drift in experimental
488 conditions. ~~(B) (B)~~ Boron content of cultured *T. weissflogii* diatom opal as a function of pH labelled
489 according to pCO₂. A least squares regression with 95% confidence interval is also shown. ~~(C) T.~~
490 *weissflogii* opal δ¹¹B against pH of each treatment demonstrating a statistically significant negative
491 relationship. Diatom data is labelled according to pCO₂ treatment. ~~(C) Boron content of cultured T.~~
492 *weissflogii* diatom opal as a function of pH (using left-axis), labelled according to pCO₂. A least
493 squares regression with 95% confidence interval is also shown. In grey (and using the right-hand

Formatted: Font: Italic

Formatted: Font: Italic

Formatted: Subscript

494 axis) are data for *T. weissflogii* from Meija et al. (2013). Note how both studies show an increase in
495 boron content with increasing pH, but absolute values differ by a factor of 2-3. Uncertainty in all
496 points is shown at the 95% confidence level. In some cases, the error bars are smaller than the
497 symbols.

498 **Figure 6:** Plots describing (A) the pH-dependent relationship between the abundance of aqueous
499 boron species, and (B) the isotopic fractionation observed between boric acid ($B(OH)_3$; red) and
500 borate ($B(OH)_4^-$; blue) at $T = 25^\circ C$ and $S = 35$.

501 **Figure 7:** (A) Back-calculated $\delta^{11}B$ of the silica deposition vesicle (SDV), and (B) the fraction of boron
502 in the SDV that is derived from external borate. In (A) the diatom $\delta^{11}B$ data are shown as grey circles
503 and the calculated $\delta^{11}B$ of the SDV as blue circles. Included in this model is an arbitrary -10 %
504 fractionation between the $\delta^{11}B$ of the SDV and the opal precipitated. The fraction of borate in the
505 SDV in (B) is a function of this assumption so these absolute values should be taken as illustrative
506 only.

507 **Figure 8:** Schematic of the model described herein for boron uptake by *T. weissflogii*. The speciation
508 behaviour and isotopic composition of boron is also shown in the insert, with the aqueous species
509 colour coded (red = boric acid, blue = borate ion). Seawater boric acid diffuses into the diatom cell
510 and the borate ion is actively transported, with HCO_3^- . While it remains unclear how boron enters
511 the silica deposition vesicle, once inside it respeciates into borate ion and boric acid, with the borate
512 ion being incorporated into the frustule. The isotopic composition of internal boron is a function of
513 external pH, which sets the isotopic composition of the incoming species, and the balance between
514 active borate ion transport and passive boric acid diffusion. The compartments are colour coded
515 according to approximate pH (scale on the right).

516 **Figure 6:** Plots describing (A) the pH dependent relationship between the abundance of aqueous
517 boron species, and (B) the isotopic fractionation observed between boric acid ($B(OH)_3$; red) and
518 borate ($B(OH)_4^-$; blue) at $T = 25^\circ C$ and $S = 35$.

519 **Figure 7:** (A) Back-calculated $\delta^{11}B$ of the silica deposition vesicle (SDV), and (B) the fraction of boron
520 in the SDV that is derived from external borate. In (A) the diatom $\delta^{11}B$ data are shown as grey circles
521 and the calculated $\delta^{11}B$ of the SDV as blue circles. Included in this model is an arbitrary -10 %
522 fractionation between the $\delta^{11}B$ of the SDV and the opal precipitated. The fraction of borate in the
523 SDV in (B) is a function of this assumption so these absolute values should be taken as illustrative
524 only.

525
526
527

Formatted: Font: Not Bold

Formatted: Indent: Left: 0 cm

Formatted: Font: Italic

Formatted: Subscript

Formatted: Superscript

528 **Tables**

529

Treatment	pCO ₂ (ppm)	2σ	pH	2σ	DIC (μM)	2σ	HCO ₃ ⁻ (μM)	2σ	Growth rate (d ⁻¹)
200	125	8	8.53	0.73	1925	61	1091	59	1.03
280	244	73	8.25	0.41	2165	113	1521	260	1.03
400	267	28	8.25	0.44	2400	115	1728	107	0.96
800	809	62	7.83	0.24	2525	56	2206	69	1.01
1600	2117	40	7.48	0.08	2791	21	2628	22	1.01

530 *Table 1: Mean carbonate system parameters experienced under the average growth*
 531 *conditions as calculated for each culture treatment on the basis of the number of cells*
 532 *grown in each 24-hour period of the batch experiment.*

533

Treatment	pH (Total scale)	pH 2σ	δ ¹¹ B	δ ¹¹ B 2σ	δ ¹¹ B sw borate	[B] ppm
200	8.55	0.63	-5.51	0.21	24.20	3.15
200	8.54	0.62	-5.40	0.21	24.00	2.81
280	8.27	0.35	-5.05	0.20	20.00	3.72
280	8.18	0.25	-5.66	0.21	18.80	0.93
280	8.30	0.42	-5.79	0.21	20.50	1.04
400	8.26	0.38	-3.64	0.20	19.90	3.37
400	8.24	0.36	-3.57	0.21	19.60	1.26
400	8.25	0.36	-2.41	0.21	19.70	2.68
800	7.85	0.22	-2.93	0.19	15.40	NA
800	7.82	0.18	-2.80	0.22	15.20	0.78
800	7.82	0.20	-3.08	0.21	15.20	1.11
1600	7.48	0.06	-1.94	0.20	13.30	0.74
1600	7.48	0.07	-3.62	0.21	13.30	0.91

534 *Table 2. Treatment name and pH with δ¹¹B and [B] for cultured T. weissflogii.*

535

536

537

538

539

540 **References**

- 541 [Amo, Y. D., and Brzezinski, M. A.: THE CHEMICAL FORM OF DISSOLVED SI TAKEN UP BY MARINE](#)
542 [DIATOMS, *Journal of Phycology*, 35, 1162-1170, 10.1046/j.1529-8817.1999.3561162.x, 1999.](#)
- 543 Anagnostou, E., Huang, K.-F., You, C.-F., Sikes, E. L., and Sherrell, R. M.: Evaluation of boron isotope
544 ratio as a pH proxy in the deep sea coral *Desmophyllum dianthus*: Evidence of physiological pH
545 adjustment, *Earth Planet. Sci. Lett.*, 349-350, 251-260, 10.1016/j.epsl.2012.07.006, 2012.
- 546 Bradshaw, A. L., Brewer, P. G., Schafer, D. K., and Williams, R. T.: Measurements of total carbon dioxide
547 and alkalinity by potentiometric titration in the GEOSECS program, *Earth Planet. Sci. Lett.*, 55, 99-115,
548 [doi:10.1016/0012-821X\(81\)90090-X](#), 1981.
- 549 Branson, O.: Boron Incorporation into Marine CaCO₃, in: *Boron Isotopes: The Fifth Element*, edited
550 by: Marschall, H., and Foster, G., Springer International Publishing, Cham, 71-105, 2018.
- 551 Brown, P. H., Bellaloui, N., Wimmer, M. A., Bassil, E. S., Ruiz, J., Hu, H., Pfeffer, H., Dannel, F., and
552 Romheld, V.: Boron in plant biology, *Plant Biology*, 4, 205-223, 2002.
- 553 Carroll, R. L., Kuchenhoff, H., Lombard, F., and Stefanski, L. A.: Asymptotics for the SIMEX Estimator in
554 Nonlinear Measurement Error Models, *Journal of the American Statistical Association*, 91, 242-250,
555 1996.
- 556 Chalk, T. B., Hain, M. P., Foster, G. L., Rohling, E. J., Sexton, P. F., Badger, M. P. S., Cherry, S. G.,
557 Hasenfratz, A. P., Haug, G. H., Jaccard, S. L., Martínez-García, A., Pälike, H., Pancost, R. D., and Wilson,
558 P. A.: Causes of ice age intensification across the Mid-Pleistocene Transition, *Proceedings of the*
559 *National Academy of Sciences*, 10.1073/pnas.1702143114, 2017.
- 560 Dickson, A. G.: Thermodynamics of the dissociation of boric acid in synthetic seawater from 273.15 to
561 318.15 K, *Deep Sea Research Part A. Oceanographic Research Papers*, 37, 755-766, [doi:10.1016/0198-](#)
562 [0149\(90\)90004-F](#), 1990.
- 563 [Dickson, A. G., Sabine, C. L. and Christian, J. R., Eds.: SOP 1: Water sampling for the parameters of the](#)
564 [oceanic carbon dioxide system, in *Guide to Best Practices for Ocean CO₂ Measurements*, PICES Special](#)
565 [Publication 3, Chapter 4, North Pacific Marine Science Organization, Sidney, BC, Canada, 2007.](#)
- 566 Dordas, C., and Brown, P. H.: Permeability of boric acid across lipid bilayers and factors affecting it, *J.*
567 *Membr. Biol.*, 175, 95-105, 2000.
- 568 Foster, G. L.: Seawater pH, pCO₂ and [CO₃²⁻] variations in the Caribbean Sea over the last 130 kyr: A
569 boron isotope and B/Ca study of planktic foraminifera, *Earth Planet. Sci. Lett.*, 271, 254-266, 2008.

570 Foster, G. L., Pogge von Strandmann, P. A. E., and Rae, J. W. B.: Boron and magnesium isotopic
571 composition of seawater, *Geochemistry Geophysics Geosystems*, 11, Q08015,
572 doi:08010.01029/02010GC003201, 2010.

573 Gray, W. R., Rae, J. W. B., Wills, R. C. J., Shevenell, A. E., Taylor, B., Burke, A., Foster, G. L., and Lear, C.
574 H.: Deglacial upwelling, productivity and CO₂ outgassing in the North Pacific Ocean, *Nature*
575 *Geoscience*, 11, 340-344, 10.1038/s41561-018-0108-6, 2018.

576 Guerrot, C., Milot, R., Robert, M., and Negrel, P.: Accurate and high-precision determination of boron
577 isotopic ratios at low concentration by MC-ICP-MS (Neptune), *Geostandards and Geoanalytical*
578 *Research*, 35, 275-284, 2010.

579 Hasle, G. R., and Fryxell, G. A.: The genus *Thalassiosira*: some species with a linear areola array,
580 *Proceedings of the Fourth Symposium on Recent and Fossil Marine Diatoms*, Oslo, 1977, 15-66,

581 Hemming, N. G., and Hanson, G. N.: Boron isotopic composition and concentration in modern marine
582 carbonates, *Geochimica et Cosmochimica Acta*, 56, 537-543, 1992.

583 Hendry, K. R., and Andersen, M. B.: The zinc isotopic composition of siliceous marine sponges:
584 Investigating nature's sediment traps, *Chem. Geol.*, 354, 33-41, 2013.

585 Henehan, M. J., Rae, J. W. B., Foster, G. L., Erez, J., Prentice, K. C., Kurcera, M., Bostock, H. C., Martinez-
586 Boti, M. A., Milton, J. A., Wilson, P. A., Marshall, B., and Elliott, T.: Calibration of the boron isotope
587 proxy in the planktonic foraminifera *Globigerinoides ruber* for use in palaeo-CO₂ reconstruction, *Earth*
588 *Planet. Sci. Lett.*, 364, 111-122, 10.1016/j.epsl.2012.12.029, 2013.

589 Henehan, M. J., Foster, G. L., Bostock, H. C., Greenop, R., Marshall, B., and Wilson, P. A.: A new boron
590 isotope-pH calibration for *Orbulina universa*, with implications for understanding and accounting for
591 vital effects, *Earth Planet. Sci. Lett.*, 454, 282-292, 10.1016/j.epsl.2016.09.024, 2016.

592 Honisch, B., and Hemming, N. G.: Surface ocean pH response to variations in pCO₂ through two full
593 glacial cycles, *Earth Planet. Sci. Lett.*, 236, 305-314, 2005.

594 Horn, M. G., Robinson, R. S., Rynearson, T., and Sigman, D. M.: Nitrogen isotopic relationship between
595 diatom-bound and bulk organic matter of cultured polar diatoms, *Paleoceanography*, 26, 1-12, 2011.

596 Ishikawa, T., and Nakamura, E.: Boron isotope systematics of marine sediments, *Earth Planet. Sci. Lett.*,
597 117, 567-580, 1993.

598 Keller, M. D., Selvin, R. C., Claus, W., and Guillard, R. R. L.: Media for the culture of oceanic
599 ultraplankton, *Journal of Phycology*, 23, 633-638, 1987.

600 Kolodny, Y., and Chaussidon, M.: Boron isotopes in DSDP cherts: Fractionation and diagenesis, The
601 Geochemical Society Special Publications, 9, 1-14, 2004.

602 Koning, E., Gehlen, M., Flank, A.-M., Calas, G., and Epping, E.: Rapid post-mortem incorporation of
603 aluminium in diatom frustules: evidence from chemical and structural analyses, Mar. Chem., 106, 208-
604 222, 10.1016/j.marchem.2006.06.009, 2007.

605 Lee, K., Kim, T.-W., Byrne, R. H., Millero, F. J., Feely, R. A., and Liu, Y.-M.: The universal ratio of boron
606 to chlorinity for the North Pacific and North Atlantic oceans, Geochimica et Cosmochimica Acta, 74,
607 1801-1811, [doi:10.1016/j.gca.2009.12.027](https://doi.org/10.1016/j.gca.2009.12.027), 2010.

608 [Lemarchand, D., Gaillardet, J., Gopel, C., and Manhès, G.: An optimized procedure for boron
609 separation and mass spectrometry analysis for river samples, Chem. Geol., 182, 323-334, 2002.](#)

610 Leonardos, N., and Geider, R. J.: Elevated atmospheric carbon dioxide increases organic carbon
611 fixation by *Emiliania huxleyi* (haptophyta), under nutrient-limited high-light conditions, Journal of
612 Phycology, 41, 1196-1203, 10.1111/j.1529-8817.2005.00152.x, 2005.

613 Lewin, J.: Boron as a growth requirement for diatoms, Journal of Phycology, 2, 160-163,
614 10.1111/j.1529-8817.1966.tb04616.x, 1966.

615 Lueker, T. J., Dickson, A. G., and Keeling, C. D.: Ocean $p\text{CO}_2$ calculated from dissolved inorganic carbon,
616 alkalinity, and equations for K1 and K2: validation based on laboratory measurements of CO_2 gas and
617 seawater at equilibrium Mar. Chem., 70, 105-119, [doi:10.1016/S0304-4203\(00\)00022-0](https://doi.org/10.1016/S0304-4203(00)00022-0), 2000.

618 Martin, J.: Glacial-interglacial CO_2 change: The iron hypothesis, Paleoceanography, 5, 1-13, 1990.

619 Martinez-Boti, M. A., Marino, G., Foster, G. L., Ziveri, P., Henehan, M. J., Rae, J. W. B., Mortyn, P. G.,
620 and Vance, D.: Boron isotope evidence for oceanic carbon dioxide leakage during the last deglaciation,
621 Nature, 518, 219-222, 10.1038/nature14155, 2015.

622 Mejia, L. M., Isensee, K., Menendez-Vicente, A., Pisonero, J., Shimizu, N., Gonzalez, C., Monteleone, B.
623 D., and Stoll, H.: B content and Si/C ratios from cultured diatoms (*Thalassiosira pseudonana* and
624 *Thalassiosira weissflogii*): Relationship to seawater pH and diatom carbon acquisition, Geochimica et
625 Cosmochimica Acta, 123, 322-337, 10.1016/j.gca.2013.06.011, 2013.

626 Ni, Y., Foster, G. L., and Elliott, T.: The accuracy of $\delta^{11}\text{B}$ measurements of foraminifers, Chem. Geol.,
627 274, 187-195, 2010.

628 Pearson, P. N., and Palmer, M. R.: Atmospheric carbon dioxide concentrations over the past 60 million
629 years, Nature, 406, 695 - 699, 2000.

Formatted: Font: Italic

Formatted: Subscript

Formatted: Subscript

630 Pfeffer, H., Daniel, F., and Romheld, V.: Boron compartmentation in roots of sunflower plants of
631 different boron status: A study using the stable isotopes ¹⁰B and ¹¹B adopting two independent
632 approaches *Physiol. Plant.*, 113, 346-351, 2001.

633 Rae, J. W. B., Foster, G. L., Schmidt, D. N., and Elliott, T.: Boron isotopes and B/Ca in benthic
634 foraminifera: proxies for the deep ocean carbonate system, *Earth Planet. Sci. Lett.*, 302, 403-413,
635 2011..

636 [R Core Team \(2018\). R: A language and environment for statistical computing. R Foundation](#)
637 [–for Statistical Computing, Vienna, Austria. URL <https://www.R-project.org/>.](#)

638 Sigman, D. M., and Boyle, E. A.: Glacial/Interglacial variations in atmospheric carbon dioxide, *Nature*,
639 407, 859-869, 2000.

640 Sigman, D. M., Hain, M. P., and Haug, G. H.: The polar ocean and glacial cycles in atmospheric CO₂
641 concentration, *Nature*, 466, 47-55, doi:10.1038/nature09149, 2010.

642 Sosdian, S. M., Greenop, R., Hain, M. P., Foster, G. L., Pearson, P. N., and Lear, C. H.: Constraining the
643 evolution of Neogene ocean carbonate chemistry using the boron isotope pH proxy, *Earth Planet. Sci.*
644 *Lett.*, 248, 362-376, doi:10.1016/j.epsl.2018.06.017, 2018.

645 Swann, G. E. A., Pike, J., Snelling, A. M., Leng, M. J., and Williams, M. C.: Seasonally resolved diatom
646 $\delta^{18}\text{O}$ records from the West Antarctic Peninsula over the last deglaciation, *Earth Planet. Sci. Lett.*, 364,
647 12-23, 10.1016/j.epsl.2012.12.016, 2013.

648 Tipper, E. T., Galy, A., and Bickle, M.: Calcium and magnesium isotope systematics in rivers draining
649 the Himalaya-Tibetan-Plateau region: Lithological or fractionation control?, *Geochimica et*
650 *Cosmochimica Acta*, 72, 1057-1075, 2008.

651 [Tortell, P. D., Martin, C. L., and Corkum, M. E.: Inorganic carbon uptake and intracellular assimilation](#)
652 [by subarctic Pacific phytoplankton assemblages, *Limnology and Oceanography*, 51, 2102-2110,](#)
653 [10.4319/lo.2006.51.5.2102, 2006.](#)

654 van Heuven, S., Pierrot, D., Rae, J. W. B., Lewis, E., and Wallace, D. W. R.: MATLAB Program Developed
655 for CO₂ System Calculations, doi:10.3334/CDIAC/otg.CO2SYS_MATLAB_v1.1, 2011.

656 Vogl, J., and Rosner, M.: Production and certification of a unique set of isotope and delta reference
657 materials for boron isotope determination in geochemical, environmental and industrial materials,
658 *Geostandards and Geoanalytical Research*, 36, 161-175, 2012.

Formatted: Font: 11 pt

Formatted: Line spacing: 1.5 lines

Formatted: Font: 11 pt

Formatted: Font: Symbol

Formatted: Superscript

Formatted: Subscript

659 [Vrieling, E. G., Gieskes, W. W. C., and Beelen, T. P. M.: Silicon deposition in diatoms: control by pH](#)
660 [inside the silicon deposition vesicle, Journal of Phycology, 35, 548-559, 10.1046/j.1529-](#)
661 [8817.1999.3530548.x, 1999.](#)

662 [Zeebe, R. E., Sanyal, A., Ortiz, J. D., and Wolf-Gladrow, D. A.: A theoretical study of the kinetics of the](#)
663 [boric acid-borate equilibrium in seawater, Mar. Chem., 73, 113-124, 2001.](#)

664

← **Formatted:** EndNote Bibliography, Left, Indent: Left: 0
cm, Hanging: 1.27 cm, Space After: 0 pt, Line spacing:
single